Chapter 1

TOWARDS AN INTEGRATED OIL SPILL SYSTEM: FROM MODELLING TO THE DECISION SUPPORT TOOL

***Juan Manuel Sayol*[1,*], *Pau Balaguer*[2], *Daniel Conti*[1], *Ana Rietz*[3], *Marcos García-Sotillo*[4], *Gonzalo Simarro*[5], *Joaquín Tintoré*[1,2] *and Alejandro Orfila*[1]**

[1]IMEDEA(CSIC-UIB). Miquel Marqués, Esporles, Spain
[2]ICTS SOCIB. Ed. Naorte, Parc Bit, Palma de Mallorca, Spain
[3]Sociedad de Salvamento y Seguridad Marítima. Fruela, Madrid, Spain
[4]Puertos del Estado. Avda. del Partenón, Madrid, Spain
[5]ICM (CSIC). Pass. Barceloneta, Barcelona, Spain

Abstract

In this chapter, we present a state-of-the-art system developed to manage oil spills crisis at the coastal areas of the Balearic Islands Archipelago. Specifically, we introduce a first version of an Integrated Decision Support System (IDSS) to response against oil spill emergencies which combines a numerical tool for tracking the spill (or objects) at the sea surface, *i.e.* the physical-geomorphological component, with a GIS tool containing the environmental and human variables. This system provides in real time the areas of probability of a spill, the potential impacts at the shore,

*E-mail address: jsayol@imedea.uib-csic.es

the uses of the affected coasts and the resources available in the surrounding areas.

Keywords: Oil Spill, Numerical Modelling, Operational Oceanography, Environmental Sensitivity Index, Search and Rescue

1. Introduction

Pollution at sea as a consequence of accidental and/or illegal spills is among the largest threats to the marine environment. Spills involving oil or hazardous materials cause every year large economical and ecological damages that, depending on the severity of the spill, its nature and the affected environment, could require decades to be recovered [1]. In the last years, the large number of incidents involving oil tankers, offshore platforms or oil pipelines resulted in an increasing concern among stakeholders and scientists on the need of developing accurate and reliable tools to forecast the evolution of those spills in the ocean [2–10]. To prevent the impact of oil spills in the environment, response plans recommend continuously monitoring the ocean and the use of forecasting systems based on Operational Oceanography to get routinely information from observations and models [11–13].

Operational systems can be composed by numerical models and/or observational platforms that provide the wind conditions and the Eulerian velocities of the ocean, which constitutes the basic information of any operational model for oil spill and Search and Rescue (SaR) operations. The evolution of the spill is then assessed using a Lagrangian model with the Operational system. Besides, the establishment of environmental sensitivity of the coasts is a key issue not only for protecting these areas in front accidental or illegal spills but also as a crucial element to make recognised the actuations that the Operational Agencies have to take in front of a potential crisis. Errors in the predicted trajectories of drifting objects are common and minimising them constitutes a very active area in Operational Oceanography where initiatives to improve both oceanic/atmospheric Operational systems and LPTAs (Lagrangian Particle Tracking Algorithms) are being undertaken [7]. The main sources of errors in oil spills and SaR operations are the result of the intrinsic complexity of the ocean dynamics and can be summarized as follows:

i) The Navier-Stokes equations governing the physics of the ocean are nonlinear and therefore, due to the chaotic nature of the ocean small variations

of the initial conditions will provide large deviation of the forecast fields that will increase with time.

ii) Operational models for ocean and atmospheric forecasting do not resolve the small scale but they parametrize the turbulent motions. In other words, no information at the sub-grid scale is provided.

iii) At the first stages of a real crisis the exact position of the accident is usually unknown resulting in wrong initial conditions for the forecasting model.

iv) The drift of an object on the ocean surface depends on the area exposed to wind and its angle of attack. These influences are usually included in the wind drag coefficient which is empirically determined sometimes after a trial-error process.

To mitigate to some extent these challenges, LPTA based models usually follow a stochastic approach [14, 15]: the uncertainty in the unknown parameters is quantified either in terms of a probability distribution or by any of the usual optimization procedures minimizing an error against available real ocean data (*e.g.* using drifters or HF-radars). However, the requirement of an online real time response, restricts the model presented in this chapter to spills at the ocean surface. Nevertheless, there are other approaches, that can study the three-dimensional processes including also chemical reactions, weathering, mechanical spreading and vertical movements but they are more computational expensive (*e.g.* [8, 9]).

The establishment of the Environmental Sensitivity (ES) of the coastline has its origins in the second half of the 70's of past century when the first classifications were conducted according to the behaviour of coastal habitats as response to hydrocarbons spills. The first examples were applied on the coasts of the USA where the Agency Responsible for oil spill mitigation, NOAA, outlined the main guidelines and criteria for elaborating sensitivity maps in order to set the Environmental Sensitivity Index (ESI). ESI is based on three major components: i) physical-geomorphological, ii) biological and iii) human use resources. These variables determine the resilience of coastal areas, understood as the ability for self-recovering after an oil spill accident. The usefulness of the ESI of a specific shoreline as a decision support tool resides in constructing hybrid forecasting systems (met-ocean models) combined together with the coastal characteristics [16].

2. Ocean Component

The dynamics of one spill at the sea surface depends on the sum of the forces acting on it. For one Lagrangian particle p, is given by the combined effect of waves, wind and currents. Neglecting viscous effects, the total velocity $\dot{\mathbf{x}}_p = \mathrm{d}\mathbf{x}_p/\mathrm{d}t$ can be decomposed as,

$$\dot{\mathbf{x}}_p(\mathbf{x}, t) = \mathbf{u}_p^{adv}(\mathbf{x}, t) + \mathbf{u}_p^{dif}(\mathbf{x}, t), \tag{1}$$

being $\mathbf{u}_p^{adv}$ and $\mathbf{u}_p^{dif}$ the advective and diffusive components of $\dot{\mathbf{x}}_p$. The advective component of the Eulerian velocity can be readily obtained from an ocean operational system as a combination of surface ocean currents ($\mathbf{u}_p^{curr}$), wave induced currents ($\mathbf{u}_p^{waves}$) and wind speed ($\mathbf{u}_p^{wind}$),

$$\mathbf{u}_p^{adv} = \mathbf{u}_p^{curr} + \mathbf{u}_p^{waves} + \gamma \mathbf{u}_p^{wind}, \tag{2}$$

where γ is a drag coefficient that depending on the object to track, spill type, shape, wind intensity and accuracy of ocean currents takes a value between 0.025 to 0.044 with a mean value of 0.03 [17]. The above can be applied for forecasting or diagnostic analysis as long as ocean currents, wave induced currents and wind speed are obtained from predictive or observational systems.

The wave induced currents are derived from the weakly non-linear wave propagation Stokes theory,

$$\mathbf{u}_p^{waves}(\mathbf{x}_p) = \frac{H^2\omega^2}{8c}\frac{\mathbf{k}}{k}, \tag{3}$$

where H is the wave height, $\omega = 2\pi/T$ the wave angular frequency, $c = \omega/k$ the wave celerity, $\mathbf{k}$ is the vector wave number and k its module ($k = \omega^2/g$).

Leaving aside the treatment of the diffusive component of the velocity, which will be addressed below, under this deterministic approach, the two-dimensional position of the particle at the ocean surface can be computed by integrating the velocity given by Eq. (1):

$$\mathbf{x}_p(t+\delta t) = \mathbf{x}_p(t) + \int_t^{t+\delta t} \mathbf{u}_p^{adv}(\mathbf{x}_p, t)dt + \int_t^{t+\delta t} \mathbf{u}_p^{dif}(\mathbf{x}_p, t)dt, \tag{4}$$

with $\mathbf{x}_p(t) = (lat,\ lon)$ the position at time t. The last term in the right hand side of Eq. (4) represents the diffusive component of the velocity field and is

the result of turbulent processes of unresolved scales. As will be discussed in the following sections, the presented model introduces in the diffusion uncertainties derived from inaccuracies of the Operational numerical models or due to incorrect initial location.

2.1. Ocean Modelling Subsystem

As stated, the core for a LPTA is composed by an Operational system which provides a regular basis wind, waves and currents on a specific area. Many Operational Systems (both under an observational or numerical perspectives) are available around the globe such as the MyOcean MED system [19, 20]. In the current version of the system we use the Western Mediterranean OPerational model, WMOP that is a regional configuration for the Western Mediterranean Sea of the Regional Ocean Modeling System ocean model (WMOP/ROMS) although it can operate with any of the operational ocean forecasting systems available in the area such as the MyOcean IBI Ocean Forecast Service (further information on the IBI system and its products in `www.myocean.org` and on the IBI quality assessment in [21]). WMOP is operated by the Balearic Islands Coastal Observing System (`ww.socib.es`) and provides operationally ocean currents every 3 hours for a 3 days horizon [22]. The area under study covers the Balearic Sea extending from 5.8° W to 9.2° E and from 34.9° N to 44.7° N (see Figure 1). The grid has 631×539 (N_x, N_y) nodes with a resolution of $\sim 1.8\,\mathrm{km}$, allowing a good sampling of the first baroclinic Rossby radius of deformation (about $10 - 15\ \mathrm{km}$) throughout the whole area [23].

2.2. Diffusivity

Following [29–31] the diffusive term can be computed as,

$$\int_t^{t+\delta t} u_j^{dif}(\mathbf{x}, t)dt = R_j\sqrt{6D\delta t}, \quad j = 1,\ 2 \tag{5}$$

with $R_j(\mathbf{x}, t)$ a random number between in $(-1, 1)$ and $D(\mathbf{x})$ the diffusivity to be empirically determined.

The random walk term in Eq. (5) has been solved by inferring the value of the diffusivity D at the ocean surface for the time scales of interest. This term is usually taken spatially and temporally constant and different values are found for a specific regime (referred as eddy diffusivity in the literature) for an

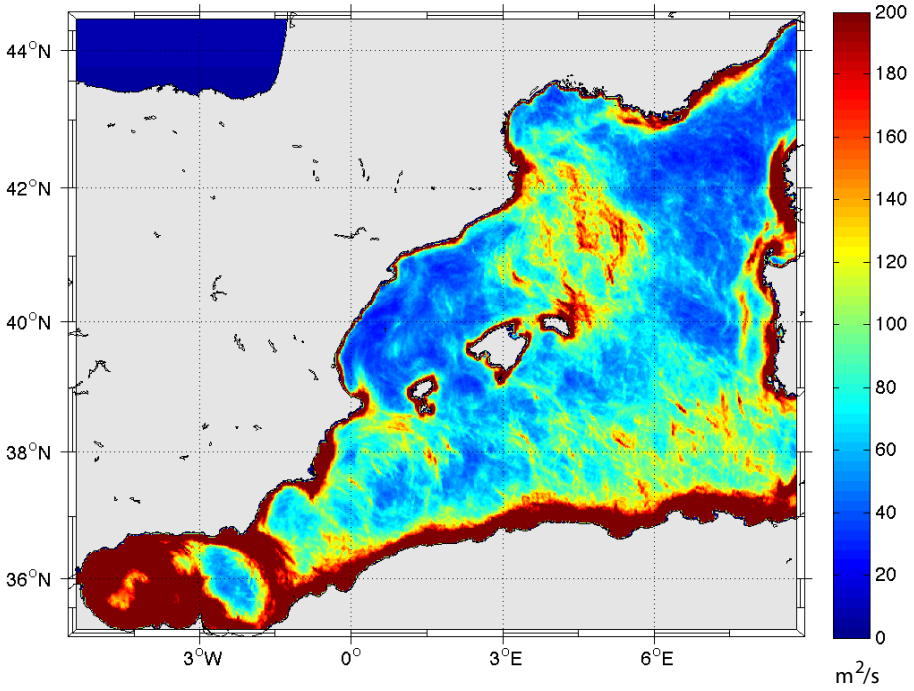

Figure 1. Geographical coverage of the numerical model. Values in the plot correspond to Western Mediterranean Sea averaged numerical diffusivity for the period January 2009-December 2011.

specific area [24]. [25] analysed the role of diffusion in the Western Mediterranean by measuring the error in the computation of Finite Size Lyapunov Exponents by changing the resolution of the model data. These authors found that diffusion introduces small scale irregularities on the trajectories, and also substantial dispersion at large scales. [18, 26] through the deployment of several surface drifters in a coastal region studied the spatial and temporal variability of diffusivity showing the different dispersion regimes in accordance with other authors [27, 28]: an exponential regime at small separations, a ballistic regime at a mesoscale range and a diffusive range at asymptotic distances.

Errors in the prediction of trajectories given by the LPTA will mainly be the result of wrong or poorly solved ocean fields provided by the Operational model

it is reasonable to compute diffusion directly from these data. Here, we have assumed the diffusivity in our model as the result of inaccuracies in the ocean model and constant in time but grid dependent. Its value is estimated directly from model data as follows. A neutrally buoyant particle was placed daily at each grid point for the period between January 2009 and December 2011 and advected during 24 hours using the velocity fields derived from the daily re-initialization and from the daily forecast. For each grid point this distance was temporally averaged and the numerical diffusivity obtained as,

$$D(lon, lat) = \frac{\epsilon^2(lon, lat)}{\delta t} \tag{6}$$

being $\delta t = 86400$ s. This pseudo-diffusivity is the result of numerical uncertainties and introduces in the LPTA the stochastic nature of the current field. For the operational model, we have temporally averaged the three year diffusivity data (see Figure 1) producing a map for the Western Mediterranean area. Larger values of diffusivity are located in the more dynamical regions (*i.e.* Alboran Sea, Algerian current, Liguro-Provenzal current as well as around the shelf seas) with values over $15\,\mathrm{m}^2/\mathrm{s}$. The influence of the northern winds in the Gulf of Lions and the northern Catalan coast also increase the value of the diffusivity. On average, in the Western Mediterranean $D \approx 10\,\mathrm{m}^2/\mathrm{s}$ which has also been suggested for the eddy diffusivity in other oceanic areas, with values oscillating between $1 - 200\,\mathrm{m}^2/\mathrm{s}$ [17].

2.3. Probability Domain

The chaotic nature of ocean will result in inaccuracies of the predicted fields from both the velocity data provided by the Operational model as well as those in the LPTA. Besides, at the initial stages of spill accidents the exact spill location is not always well determined resulting in large errors in predictions.

To delimit these constrains, this approach computes the contours of probability of the final positions of a group of neutrally buoyant particles instead of providing the individual track of them. A set of particles is distributed around a spill location in a circular area of small radius defined by the user. The path for each particle is solved and the probability density function of them computed by a Gaussian kernel estimator [32] as,

$$\widehat{f}_{ker}(x, y) = \frac{1}{2\pi N h_x h_y} \sum_{i=1}^{N} \prod_{j=1}^{2} \exp\left(-\frac{1}{2}\left(\frac{x_j - X_{ij}}{h_j}\right)\right), \tag{7}$$

where N is the number of particles launched, x_j is the final position ($j = 1$ longitude and $j = 2$ latitude) of the particles, X_{ij} is the $j - th$ component of the $i - th$ observation and h_j is the bin width given by the normal reference rule, e.g.,

$$h_j = \left(\frac{1}{N}\right)^{1/6} \sigma_j, \tag{8}$$

being σ_j the standard deviation of final positions.

With this methodology the model provides to the user contours of accumulated probability at the desired confidence intervals (e.g., 90%, 75%, 50%) which coincide with the isolines of the kernel.

2.4. Model Validation

To test the numerical component developed, a real experiment was carried out during October 2012 in the frame of the European Union project TOSCA. In collaboration with SASEMAR, Puertos del Estado and SOCIB, some drifters were deployed in the Balearic Islands region, in the middle of the Ibiza Channel. To illustrate how the system works, it has been simulated the evolution during 24 hours for one of the drifters that was deployed at $(\mathrm{lon}, \mathrm{lat}) = (0.8097^\circ\,\mathrm{E}, 38.8463^\circ\,\mathrm{N})$. The drifter transmitted its position through GPS from October 25^{th} 2012 to January 23^{rd} 2013, travelling hundreds of km until reaching the Strait of Sicily (see Figure 3(a), black line). A zoom highlighting the trajectory is displayed in Figure 3(b), where the red line shows the trajectory of the drifter corresponding to the period of simulation, from 25^{th} October at 21:30 UTM to 26^{th} October at 21:30 UTM. The blue and green areas represent the initial distribution of the virtual particles and the final position after 24 hours of simulation respectively. The Gaussian kernel of density probability computed from the final distribution of particles is shown in Figure 3(c) and the resulting contours of accumulated probability derived from the kernel are shown in Figure 3(d) where contours correspond to the 50% in black and 70% in grey of accumulated probability. As seen, the drifter position is inside the contour of 50% of accumulated probability (blue cross), which is also in good agreement with previous results presented in [10]. At this point, we want to remark that several tests were made to check the proper numerical algorithm, the number of initial particles and the integration time step in order to get the best combination of accuracy and computational time. From these tests, we conclude that no

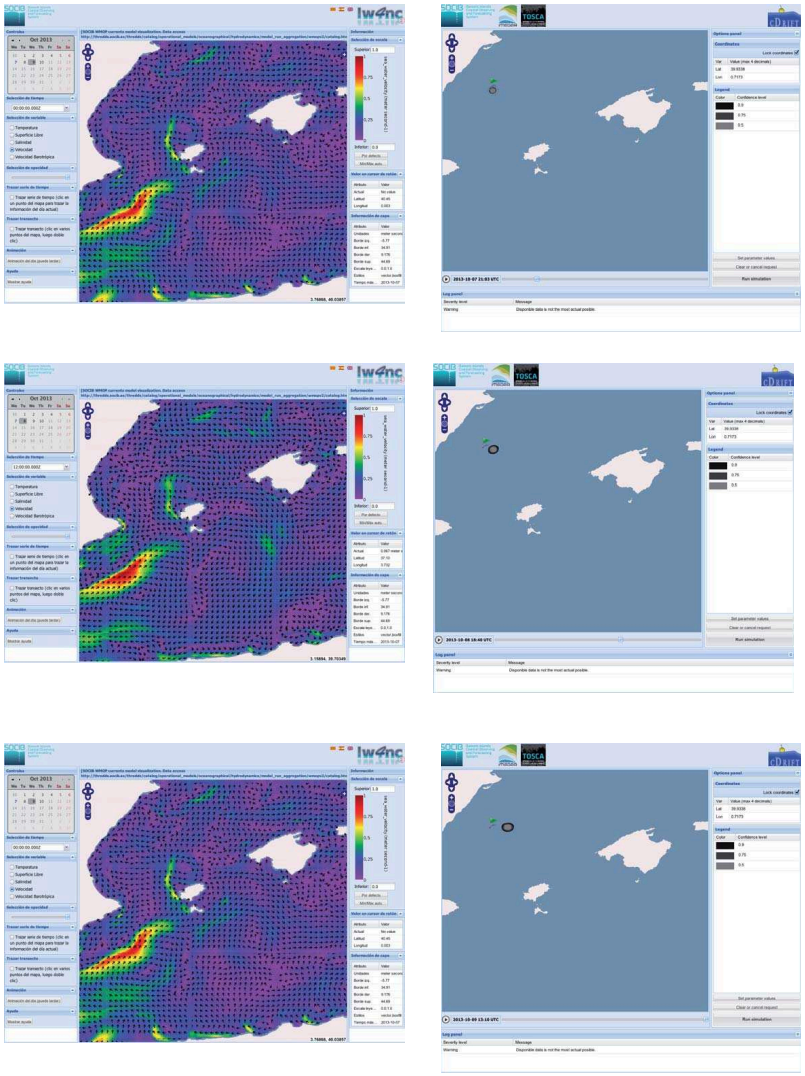

Figure 2. Daily forecast of contours of 50 (black), 70 (gray) and 90 (gray dashed) accumulated probability of spill incidence for a spill at 39.93° N and 0.72° E on October 7^{th} 2013 (right panels). On the left the oceanographic conditions as given by the numerical model.

differences are obtained for the final probability distribution when using more than 200 virtual particles/simulation.

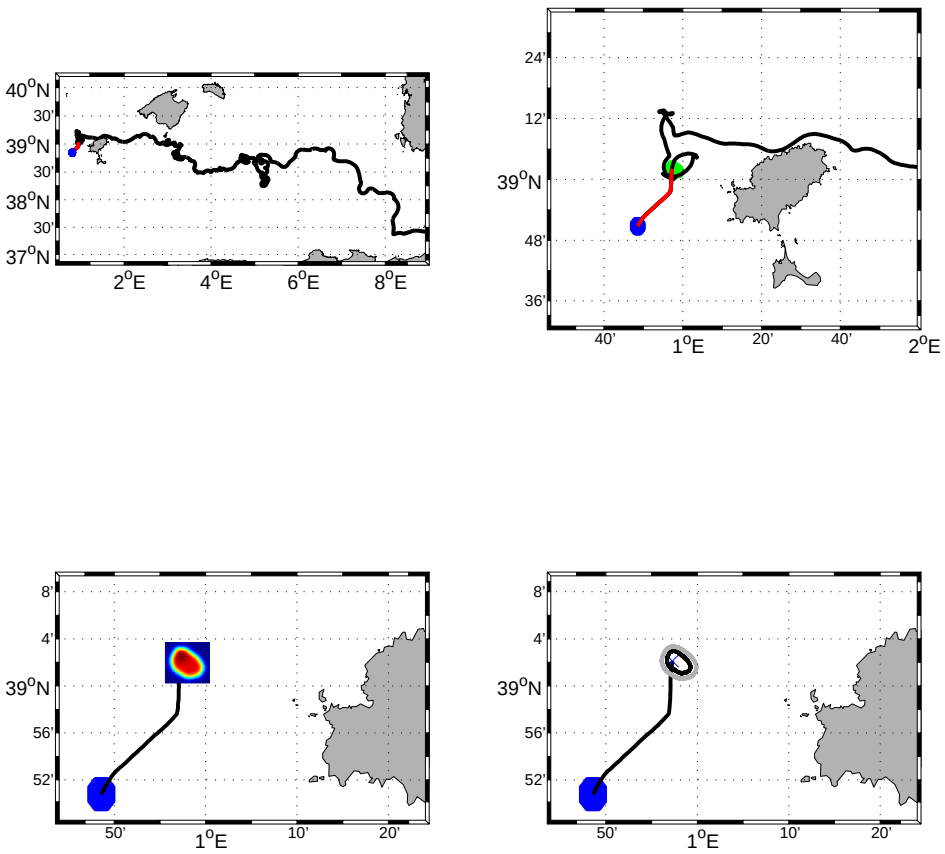

Figure 3. (a) Drifter trajectory between October 25^{th}, 2012 to January 23^{rd}, 2013. (b) Trajectory of the drifter for the numerical experiment corresponding to 25^{th} October at 21:30 UTM to 26^{th} October at 21:30 UTM (red). The initial and final distribution of the virtual particles are displayed in blue and green respectively. (c) The kernel of density probability computed for the final distribution of particles. (d) The corresponding contours of accumulated probability. The black line correspond to the 50% probability contour and the grey to the 70%.

3. Decision Support System

3.1. Environmental Sensitivity Index

Shoreline Environmental Sensitivity Maps have been developed in many coastal areas of the world with examples in the most populated areas of North, South and Central America, Europe, Mediterranean Sea Region, Middle East, Indian Ocean islands, Oceania, Africa, Asia and the Pacific [33–44, 47].

The establishment of the ES of the coastline appears as a dynamic and continuous task due to the frequent changes that occur in the shoreline (variations in roughness of the coastline due to erosion or human action -*i.e.* ports, jetties, groynes, etc.-. The changes in the coastal zone may also be due to increased knowledge about these areas from a physical and/or biogeographic vision, in this way it could provide a better understanding of the sensitivity degree. The coastline may also be related with changes of spatial planning (land use changes, population increase, restoring natural areas) that will influence the pressure on these areas (*e.g.* new infrastructure and services). In general, knowledge of the coastline is constantly evolving and natural processes and human-induced changes makes it as a dynamic space both in the socio-economic dimension as in the natural environment (physical and biotic) both in space and time.

Integrated Coastal Zone Management (ICZM) is based on the concept by which the management of resources and terrestrials and marine areas should be fully integrated as well as the ecosystems that are part of these areas. ICZM has a close relationship with Marine Spatial Planning (MSP) defined as a practical process for establishing a rational organization of the marine environment and assessment of use. The overlapping of the study areas for IZCM and MSP gives rise the concept of Integrated Coastal and Marine Management (ICMM) [45] incorporating the marine environment of the coastal area as a fundamental element. Shoreline ES gathers information of physical, bio-ecological and human use resources constituting a decision tool to manage marine pollution emergencies, and to provide extremely useful background information in a framework of ICMM [46].

3.1.1. Shoreline Classification

Physical substrate of shoreline will determine the persistence of pollutants on the coast depending on the capacity of the materials to retain them. A description of shoreline types is shown in Figure 4. The shoreline classification is

derived from 1) the height of the specific coast; 2) the exposure of the coast to the main wave climate; 3) the type of substrate; 4) the biological sensitivity degree.

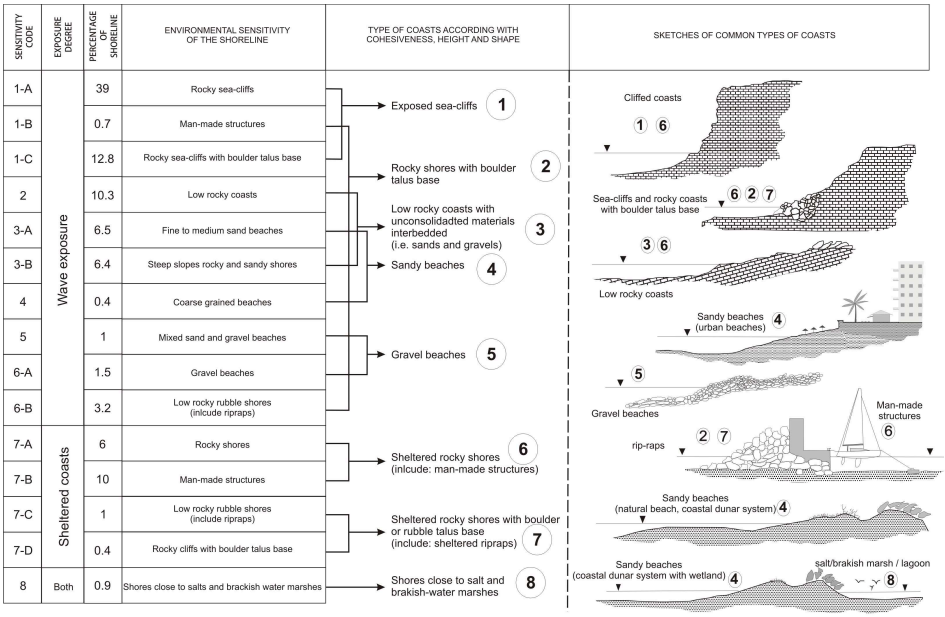

Figure 4. Description and percentage length of types of coasts of Balearic Islands according to the Environmental Sensitivity (ES). The figure represents the relationship between sensitivity degree (left), geomorphological classification (centre) and common types of coasts (right).

- Height criteria. This criteria has been determined according to the first works related to coastal geomorphology classification for the Balearic Islands [48] which establish 3 meters height as the boundary between high and low coasts. Coastal height also will determine the accessibility for cleaning up and restoration tasks in case of a contamination event. Many rocky coasts (low and high coasts) of Balearic Islands have a step-like morphology and in some cases this feature results in a supratidal/backshore strip composed by accumulation of boulders, pebbles and unconsolidated materials with other sensitivity respect the materials lo-

cated at the shoreline. Based on this, in recent field surveys we have adopted the criteria of [47] to map the parallel backshore strips or belts which may be affected due storm surges.

- Exposure degree to wave energy. Following [37, 49] there are mainly two types of coasts regarding the influence of waves. The first type corresponds to those coasts exposed to waves (high energy coasts). In these environments the spill will tend to be naturally removed. The second type correspond to sheltered coasts (low energy environments) where the spill will be gradually be removed. The degree of exposure to wave energy is determined by the degree of articulation of the coastline (capes, natural harbour, bays, coves) and bathymetry that will condition the dissipation of the wave energy allowing the arrival of wave trains to the shoreline.

- Substrate type: the most important distinction is between bedrock and unconsolidated sediments [37]. Penetration depth is controlled by grain size of the substrate and will lead the long-term biological impacts. Deepest penetrations occur in sediments from gravel sizes (< 2mm), and man-made ripraps (boulder size) that allow deeper penetration of pollutants and act as storage areas for long periods of time. Regarding the classification of beach types in relation to the grain size, it have been used previous works of textural classification for beaches of Mallorca and Menorca [50].

- Biological sensitivity. This criteria refers to the ability of the coastal environment to host different types of habitat. Indeed, coastal types are related to the morphology of the shore-in a regional context- which is not a close concept. This classification was made upon previous works and sported by aerial photographs [48].

3.1.2. Biological-Ecological Characterization

Biological and/or ecological characterization is based on the development of different degree of biological vulnerability of the coasts of the Balearic Islands. These degrees of vulnerability have been made according to the criteria based on a number of protection figures (marine and terrestrial) located at coastal areas in accordance with the Coastal Sensitivity Atlas of Finisterre Region [40]. In this task we have considered the kinds of protection at several levels: International (World Heritage status), European (Nature Network 2000), National and Regional (*e.g.* National Parks, Natural Reserves, Marine Reserves levels, among

others). In this sense, natural areas are protected because of their physical, biological and ecological elements that confers them significant vulnerability. The overlapping of maps of protected areas of Balearic Islands was made using geoprocessing tools (program ArcMap 9.2, ESRI).

3.1.3. Human Use Resources

The third component of the ES of the shoreline is the human use resources. This task is made by identifying the points/areas of interest in case of an oil spill or other pollution events. Features considered are infrastructures, equipments, services, leisure activities (*e.g.* water sports) and historical/cultural areas (including archaeological sites) of the shoreline that have to be into account in case of an oil spill because they could receive direct impact or could be damaged during the clean-up tasks and/or restoration of the shoreline.

3.2. The Balearic Islands Case

Shoreline Classification

The classification of the Environmental Sensitivity (ES) is made for the Balearic Islands coasts (Figure 5) being based on the international standard/guidelines proposed by NOAA designed for the establishment of the Environmental Sensitivity Index (ESI) [37]. The adoption of these guidelines responds to the need for standardizing the information in terms of the response to pollution and the location of sensitive resources that may be affected. ES classification, as a continuous task, had added more criteria from further studies published after the first results in 2006 (*e.g.* [47]). Classification and mapping tasks were performed using Geographic Information Systems (GIS) using ArcGIS© program by Esri. GIS allows an agile management to integrate the information according to certain attributes during emergencies and also for coastal management purposes. ES maps comprise three types of information: a) shoreline classification; b) biological-ecological characterization; and c) human use resources.

In the Balearic Islands, we have identified 8 types of coasts divided in 15 sub-types (Figure 4). The predominant types of coasts of Balearic Islands are exposed cliffs representing the 51% of the shoreline (Figure 4, types 1-A and 1-C); coasts formed by unconsolidated materials (sandy and gravel beaches) representing the 9.4% (Figure 4, types 3-A, 4, 5 and 6-A); sheltered rocky coasts (Figure 4, types 7-A, 7-B, 7-C and 7-D) representing 17.4% being the most sen-

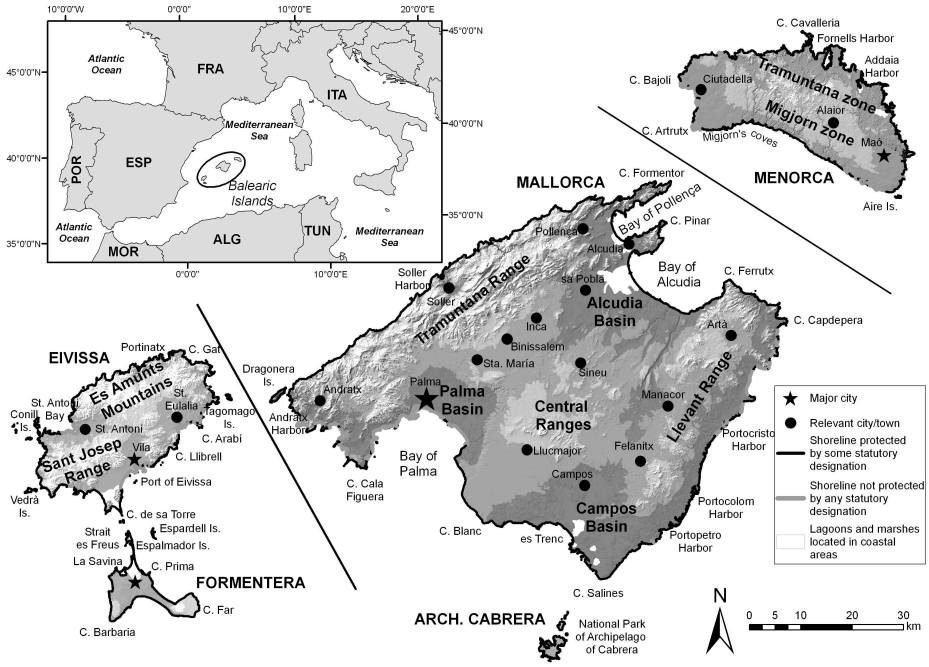

Figure 5. Location of Balearic Islands in Western Mediterranean and cartography of Balearic Islands showing main coastal toponyms, morphostructural units, cities/towns and shoreline protected by some statutory designation.

sitive shorelines (Figure 4, type 8). To be note the man-made ripraps (Figure 4, included in coasts 6-B and 7-C), that are around the 2% of the Balearic shoreline located at both sheltered and exposed energy regimes. Ripraps are coasts with high secondary porosity which permits the storage and persistence of oil (or pollutants) leading to potential long-term biological impacts and making the clean-up tasks more difficult [37].

The first ES classifications had 9 main types of coasts and 17 sub-types [51]. A reduction in the number of types of coasts was due to the suppression of sheltered sandy and gravel beaches. Beaches play an important role in the overall economy of the Balearic Islands hosting the major part of mass tourism [52]. The legend was changed due to: 1) the difficulty to establish the wave regime for all the beaches of the archipelago (around 900 sedimentary deposits have

been recognized for the whole archipelago), b) [37] determine the sensitivity of beaches according with the capability of the substrate to sustain pedestrians and machinery for cleaning-up tasks, and c) there is not a direct relationship between the degree of exposure to wave energy and biological richness, but some studies highlights the trend of sheltered beaches to have higher biodiversity, particularly regarding macrofauna [53–55]. Therefore, exposure to beaches wave energy should be considered in respect of the coastal context, depending on the exposure to waves of nearby rocky shorelines (*e.g.* beaches inside caves, enclosed bays or natural harbours). During summer 2011 a field survey was carried out in the Bay of Palma (as a pilot area). This field survey campaign, along 125 km, was intended to provide better support for decision making, in connection to clean-up and restoration tasks of the shoreline. This experiment provided detailed in-situ high resolution photographs (useful for decision makers) and some features as the existence of backshore strips (accumulation of boulders and pebbles) and litoral caves were included into the cartographic database following the indications of [47].

Biological Ecological Characterization

The overlapping of protected areas in the Balearic Islands shows that 83% of the shoreline is protected by some statutory designation and the remaining 17% mainly corresponds to consolidated urban nucleus with majority of modified coasts by man and man-made structures. All the islets were protected since 1991 by a regional law, and most of them were subsequently affected by several environmental protections (*e.g.* Natura 2000 Network) due to their high biogeographical value because of the many endemic species of flora and fauna [56]. Shorelines with higher environmental protections are located in the strait of Es Freus, between Eivissa and Formentera, Archipelago of Cabrera (National Park) and coastal domains of Serra de Tramuntana in Mallorca (Figure 5). High environmental protection it is also noticeable in the northern coasts and central stretch of southern coasts of Menorca, northeastern and southeastern coasts of Mallorca, northwestern coasts of Eivissa and the entire shoreline of Formentera (Figure 5).

Human Use Resources

It has been mapped 27 features in the coastal zone according to their vulnerability or usefulness front an oil spill. Areas with a greater availability of human

use resources are located in urban areas and especially in ports. Coastal areas with a certain lack of human use resources aimed to mitigate pollution impacts and promote environmental restoration are located in the northwestern coasts of Mallorca (Serra de Tramuntana) and Eivissa (es Amunts mountain range), and northern coasts of Menorca (Tramuntana zone) (Figure 5).

4. Results

The tools conforming the system presented in this chapter have been developed by different institutions and are continuously under upgrade. The main objective is to provide to the end user (the agencies in charge of the response in front an accident) efficient, validated and friendly tools to react with scientific knowledge in case of a spill or SaR operations. The system has been designed to be easily relocatable as well as machine independent. Moreover, requests for a specific crisis can be made by stakeholders or civil protection personnel with little oceanographic knowledge, so the interface between model and the end-users has to be as simple as possible providing the least unknown parameters undetermined. The Operational model provides surface currents, wind and wave fields for the following 72 hours at a 3 hour interval. Velocity fields (ocean surface currents and wind speed) are arranged in a cube (tensor) with dimensions ($N_x,\ N_y,\ N_t$), where $N_t = 25$ corresponds to the forecasting times of $t(\mathrm{hours}) = 0, 3, 6, ...72$, provided by the WMOP.

Presently, atmospheric, oceanic and wave models (HIRLAM, WMOP and WAM respectively) are written in Fortran as well as the LPTA module, providing data in NetCDF format. After LPTA computations the resulting probability contours are displayed by GeoJSON scripts through a web based Java interface. The end-user is allowed to select some basic parameters such as the initial position (latitude and longitude), the total advection time (up to 72 hours), the number of particles to be initially deployed or the confidence intervals to be displayed. Snapshots of the Java interface for a hypothetical spill occurring at $39.93^\circ\,\mathrm{N}$ and $0.72^\circ\,\mathrm{E}$ on October 7^{th} 2013 are shown for different times in Figure 2 (right panels). In these snapshots the specific contours correspond to the 50%, 75% and 90% of accumulated probability. The corresponding model forecast are shown in the left panels of Figure 2.

Once the spill reaches the coast a web-based map viewer displays the cartographic data related to ES of the shoreline of the Balearic Islands (Figure 6). This viewer was designed to be a decision-making tool to support the Emer-

gency Services of the Balearic Islands to response to potential oil spills. This Web Map Service (WMS) tool complies with OGC (Open Geospatial Consortium) interoperability standards and the criteria of the INSPIRE directive. Data can be accessed directly through the map viewer, via Google Earth (metadata window and download KML/Z) or via WMS. Cartographic information are divided according to the three main components described above: 1) Shoreline types shown in Figure 4, 2) Biological resources (coastal protected areas by some statutory designation) and, 3) Human use resources. Oblique aerial photographs (corresponding to 4 different flights) are also included in order to help clean-up and recovery tasks (Figure 6). Each coastal stretch is related with an oblique aerial photograph and WMS also provides information on the length (m), description of the shoreline type and relevant information (*e.g.* presence of sea caves, characteristics of substrate on the backshore and variations in the legend) (Figure 6).

5. Conclusion

This Chapter presents a state-of-the-art system for the management of oil spill crisis at sea. Specifically we develop a first version of an Integrated Decision Support System (IDSS) for oil spill reaction that combines a numerical tool for tracking the spill at the ocean (the physical-geomorphological component) with a GIS tool containing the environmental and human variables.

The system is conformed by several modular components that are easily relocatable and with the objective to provide to the user, accurate and updated information on the trajectory of the spill, the sensitivity of the coast where the spill will shore and the resources available through the database linked to the GIS system. The system uses met-ocean forecast from an Ocean Operational System and provides the kernel density of the trajectories of virtual particles launched in the origin of the spill that evolve with the currents, wind and waves for the next 72 hours. When the spill reaches the coast the system uses the data from an ES system on the GIS to provide all the information about the actions that has to be taken as well as the available resources. The Lagrangian tool as well as the Environmental Sensitivity have been designed mainly for oil spills, but also could be applied to face to marine pollution accidents or SaR operations.

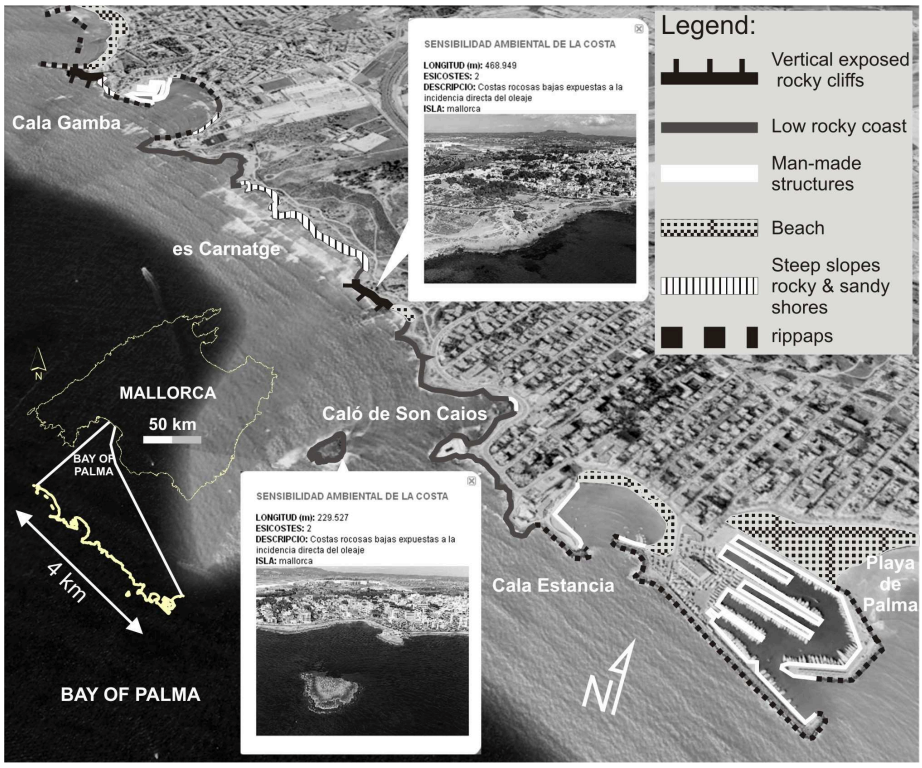

Figure 6. Example of simplified map of shoreline environmental sensitivity (ES) of a coastal stretch of Bay of Palma (Mallorca) from web-based map viewer (`http://gis.socib.es/sacosta/composer`).

Acknowledgments

Authors are indebted to ICTS-SOCIB modelling, observing and data center facilities. Field and modelling support from SASEMAR is greatly acknowledged. J.M.S. is supported by the PhD CSIC-JAE program co-funded by the European Social Fund (ESF) and CSIC. D.C. thanks the financial support from the Balearic Islands Government through a predoctoral grant co-funded by the European Social Fund (ESF). G.S. is supported by the Spanish government through the Ramón y Cajal program. Authors would like to thank financial support from MED Project MEDESS-4MS. The authors also thank financial support from

MICINN through Project 289 445 CGL2011-22964. Authors strongly thank the Government of the Balearic Islands and FEDER through the Grups Competitius program.

References

[1] Elliot, A., Jones, B., 2000. The need for operational forecasting during oil spill response. *Marine Pollution Bulletin* 40 (2), 110–121.

[2] Reed, M., Johansen, O., Brandvick, P., Daling, P., Lewis, A., Fiocco, R., Mackay, D., Prentki, R., 1999. Oil spill modeling towards the close of the 20th century: Overview of the State of the Art. *Spill Science & Technology Bulletin* 5 (1), 3–16.

[3] Sebastião, P., Soares, C. G., 2006. Uncertainty in predictions of oil spill trajectories in a coastal zone. *Journal of Marine Systems* 63, 257–269.

[4] Kirby, M., Law, R., 2010. Oil spill, Chemical spill, Impact assessment, Monitoring, Emergency response, Shipping accidents. *Marine Pollution Bulletin* 60 (6), 797–803.

[5] Wang, J., Shen, Y., 2010. Modeling oil spills transportation in seas based on unstructured grid, finite-volume, wave-ocean model. *Ocean Modelling* 35, 332–344.

[6] Neuparth, T., Moreira, S., Santos, M., Reis-Henriques, M., 2012. Review of oil and HNS accidental spills in Europe: Identifying major environmental monitoring gaps and drawing priorities. *Marine Pollution Bulletin* 64 (6), 1085–1095.

[7] Olascoaga, M., Haller, G., 2012. Forecasting sudden changes in environmental pollution patterns. *PNAS* 109 (13), 4738–4743

[8] De Dominicis M., Pinardi N., Zodiatis G., Lardner R., 2013. MEDSLIK-II, a Lagrangian marine surface oil spill model for short-term forecasting - Part 1: Theory. Geosci. *Model Dev.* 6, 1851–1869.

[9] De Dominicis M., Pinardi N., Zodiatis G., Archetti R., 2013. MEDSLIK-II, a Lagrangian marine surface oil spill model for short-term forecasting

- Part 2: Numerical simulations and validations. Geosci. *Model Dev.* 6, 1871–1888.

[10] Sayol J.M., Orfila A., Simarro G., Conti D., Renault L., Molcard A., 2014 A Lagrangian model for tracking surface spills and SaR operations in the ocean, *Environmental Modelling & Software* 52(2), 74–82.

[11] Kamachi, M., Fujii, Y., Zhou, X., 2002. Ocean data assimilation in the Tropical Pacific: A short survey. *Journal of Oceanography* 58 (5-7), 45–55.

[12] Siddorn, J., Allen, J., Blackford, J., 2007. Modelling the hydrodynamics and ecosystem of the North-West European continental shelf for operational oceanography. *Journal of Marine Systems* 65 (1-4), 417–429.

[13] Gonzalez, M., Ferrer, L., Uriarte, A., Urtizberea, A., Caballero, A., 2008. Operational Oceanography System applied to the Prestige oil-spillage event. *Journal of Marine Systems* 72, 178–188.

[14] Abascal, A., Castanedo, S., Medina, R., Liste, M., 2010. Analysis of the reliability of a statistical oil spill response model. *Marine Pollution Bulletin* 60 (11), 2099–2110.

[15] Minguez, R., Abascal, A., Castanedo, S., Medina, R., 2012. Stochastic Lagrangian trajectory model for drifting objects in the ocean. *Stoch Environ Res Risk Assess* 26 (8), 1081–1093

[16] Jordi, A., Ferrer, I., Vizoso, G., Orfila, A., Basterretxea, G., Casas, B., lvarez, A., Roig, D., Garau, B., Martnez, M., Fernndez, V., Forns, A., Ruiz, M., Forns, J.J., Balaguer, P., Duarte, C.M., Rodrguez, I., lvarez, E., Onken, R., Orfila, P., Tintor, J. 2006. Scientific management of Mediterranean coastal zone: A hybrid forecasting system for oil spill and search and rescue operations. *Marine Pollution Bulletin* 53, 361–368.

[17] ASCE, 1996. State-of-the-art review of modeling transport and fate of oil spills, ASCE committee on modeling oil spills water resources engineering division. *Journal of Hydraulic Engineering* 122 (11), 594–609.

[18] De Dominicis, M., Leuzzi G., Monti P., Pinardi N., Poulain P.-M., 2012. Eddy diffusivity derived from drifter data for dispersion model applications. *Ocean Dynamics*, 62, 1381–1398,

[19] Pinardi, N., Allen, I., Demirov, E., de Mey, P., ans A. Lascaratos, G. K., Traon, P.-Y. L., Maillard, C., Manzella, G., Tziavos, C., 2003. The Mediterranean ocean Forecasting System: first phase of implementation (1998-2001). *Annales Geophysicae* 21, 3–20.

[20] Downbrowsky, E., Bertino, L., Brassington, G., Chassignet, E., Davidson, F., Hurlburt, H., Kamachi, M., Lee, T., Martin, M., Mei, S., Tonani, M., 2009. GODAE systems in Operation. *Oceanography* 22 (3), 77–92.

[21] Maraldi, C., Chanut, J., Levier, B., Reffray, G ., Ayoub, N., De Mey, P., Lyard, F., Cailleau, S., Drevillion, M., Alvarez- Fanjul, E., García-Sotillo, M., Marsaleix, P. and the Mercator Research and Development Team. NEMO on the shelf: assessment of the Iberia Biscay Ireland configuration, 2013. *Ocean Science* 9, 745–771

[22] Tintoré, J. et al., 2013. SOCIB: The Balearic Islands Coastal Ocean Observing and Forecasting System Responding to Science, Technology and Society Needs. *Marine Technology Society Journal* 47 (1), 101–117.

[23] Send, U., Font, J., Krahmann, G., Millot, C., Rhein, M., Tintore, J., 1999. Recent advances in observing the physical oceanography of the Western Mediterranean. *Progress in Oceanography* 44, 37–64.

[24] Okubo, A., 1971. Oceanic diffusion diagrams. *Deep Sea Research* 18, 789–802.

[25] Hernandez-Carrasco, I., Lopez, C., Hernandez-Garcia, E., Turiel, A., 2012. How reliable are finite-size Lyapunov exponents for the assessment of ocean dynamics? *Ocean Modelling* 36 (4), 208–218.

[26] Mantovanelli, A., Heron, M., Heron, S., Steinberg, C., 2012. Relative dispersion of surface drifters in a barrier reef region. *Journal of Geophysical Research* 117 (C11016), 15 pp.

[27] Lacasce, J., Bower, A., 2000. Relative dispersion in the subsurface North-Atlantic. *Journal of Marine Research* 58, 863–894.

[28] Lacasce, J., Ohlmann, C., 2003. Relative dispersion at the surface of the Gulf of Mexico. *Journal of Marine Research* 61, 285–312.

[29] Ross, O., Sharples, J., 2004. Recipe for 1-D Lagrangian particle tracking models in space-varying diffusivity. *Limnology and Oceanography: Methods* 2, 289–302.

[30] Marinone, S., 2006. A numerical simulation of the two- and three-dimensional Lagrangian circulation in the northern Gulf of California. *Estuarine, Coastal and Shelf Science* 68, 93–100

[31] Marinone, S., Lavin, M., Paris-Sierra, A., 2011. A quantitative characterization of the seasonal Lagrangian circulation of the Gulf of California from a three-dimensional numerical model. *Continental Shelf Research* 31 (14), 1420–1426.

[32] Martinez, W., Martinez, A., 2002. *Computational Statistics Handbook*. Chapman and Hall. CRC, Boca Raton, Florida.

[33] Hanna, R.G.M. 1995. An approach to evaluate the application of the vulnerability index for oil spills in tropical red sea environments. *Spill Science & Technology Bulletin* 2, 171–186.

[34] Krishnan, P. 1995. Research report A geographical information system for oil spills sensitivity mapping in the Shetlands Islands (United Kingdom). *Ocean & Coastal Management* 26, 247–255.

[35] Jensen, J.R.; Halls, J.N., Michel, J.A. 1998. Systems approach to environmental sensitivity index (ESI) mapping for oil spill contingency planning and response. *Photogrammetric Engineering and Remote Sensing* 64 (10), 1003–1014.

[36] Nansingh, P., Jurawan, S. 1999. Environmental sensitivity of a tropical coastline (Trinidad, West Indies) to oil spills. *Spill Science & Technology Bulletin* 5 (2), 161–172.

[37] NOAA (National Oceanic and Atmospheric Administration). 2002. Environmental Sensivity Index Guidelines. *NOAA Technical Memorandum NOS OR&R* 11. Hazardous Materials response Division. Office of Response and Restoration. National Ocean and Atmospheric Administration & Department of Comerce United States of Amrica. 89 pp.

[38] Wieczorek, A., Dias-Brito, D., Carvarhlo-Milaneli, J.C. 2007. Mapping oil spill environmental sensitivity in Cardoso Island State Park and surroundings areas, Sao Paulo, Brazil. *Ocean & Coastal Management* 50, 872–886.

[39] Assilzadeh, H., Gao, Y., Ley, J.K.. 2009. Coastal zone mapping for oil spill emergency management. *Sea Technology* 50 (9), 33-34.

[40] Castanedo, S., Juanes, J.A., Medina, R., Puente, A., Fernández, F., Olabarrieta, M., Pombo, C. 2009. Oil spill vulnerability assessment integrating physical, biological and socio-economical aspects: Application to the Cantabrian coast (Bay of Biscay, Spain). *Journal of Environmental Management* 91 (1), 149–159.

[41] Pincinato, F. L., Riedel, P.S., Milanelli, J.C.C. 2009. Modelling and expert GIS based on knowledge to evaluate oil spill environmental sensitivity. *Ocean & Coastal Management* 52, 479–486.

[42] Bello-Smith, A., Cerasuolo, G., Perales, J.A., Anfuso, G. 2011. Environmental sensitivity maps: the northern coast of Gibraltar Strait example. *Journal of Coastal Research* SI64, 875–879.

[43] Fattal, P., Maanan, M., Tillier, I., Rollo, N., Robin, M., Pottier, P. 2010. Coastal vulnerability to oil spill pollution: the case of Nourmoutier Island (France). *Journal of Coastal Research* 26 (5), 879–887.

[44] Oyepedo, J.A., Adeofun, C.O. 2011. Environmental sensitivity index mapping of Lagos shoreline. *Global Nest Journal* 13 (3), 277-287.

[45] Cicin-Sain, B., Belfiore, S. 2005. Linking marine protected areas to integrated coastal and ocean management: A review of theory and practice. *Ocean & Coastal Management* 46 (11-12), 847-868.

[46] Belfiore, S., Cicin-Sain, B., Ehler, C., Editors. 2004. *Incorporating Marine Protected Areas into Integrated Coastal and Ocean Management: Principles and Guidelines.* IUCN, Gland, Switzerland and Cambridge, UK. 38 pp.

[47] Adler, E., Inbar, M. 2007. Shoreline sensitivity to oil spills, the Mediterranean coast of Israel: assessment and analysis. *Ocean & Coastal Management* 50, 24-34.

[48] Butzer, K.W. 1962. Coastal geomorphology of Majorca. Annals of Asoc. *American Geographers* 52 (2), 191-212.

[49] Hayes, M.O. 1996. An exposure index for oiled shorelines. *Spill Science & Technology Bulletin* 3, 139-147

[50] Gómez-Pujol, L., Roig-Munar, F.X., Forns, J.J., Balaguer, P., Mateu, J. 2012. Provenance-related characteristics of beach sediments around the island of Menorca, Balearic Islands (western Mediterranean). *Geo-Mar Lett* 33, 195–208

[51] Balaguer, P., Sardá, R., Ruiz, M., Diedrich, A., Vizoso, G., Tintoré, J. 2008. A proposal for boundary delimitation for integrated coastal zone management initiatives. *Ocean & Coastal Management* 51, 806–814.

[52] Aguiló, E., Alegre, J., Sard, M. 2005. The persistence of the sun and sand tourism model. *Tourism Management* 26 (2), 219-231.

[53] McLachlan, A. 1990. Dissipative beaches and macofauna communities on exponed intertidal sands. *Journal of Coastal Research* 6 (1), 57-61.

[54] McLachlan, A., Brown, A.C. 2006. *The ecology of sandy shores.* 2on edition. Academic Press, New York, 373 pp.

[55] Sevastou, K., Lampadariou, N., Eleftheriou, A. 2011. Meiobenthic diversity in space and time: The case of harpacticoid copepods in two Mediterranean microtidal sandy beaches. *Journal of Sea Research* 6 (3), 205–214.

[56] Palmer, M., Pons, G., Cambefort, I., Alcover, J.A. 1999. Historical processes and environmental factors as determinants of inter-island differences in endemic faunas: the case of the Balearic Islands. *Journal of Biogeography* 26, 813–823.

MA